Amide-to-ester substitution as a strategy for optimizing PROTAC permeability and cellular activity

Victoria G Klein,[1,a,#] Adam G. Bond,[2,#] Conner Craigon,[2] R. Scott Lokey, [1,*] Alessio Ciulli,[2,*]

Author Affiliations:
[1] Department of Chemistry and Biochemistry, University of California Santa Cruz, Santa Cruz, CA, USA
[2] Division of Biological Chemistry and Drug Discovery, School of Life Sciences, University of Dundee, Dow Street, Dundee, DD1 5EH, Scotland, UK.

Current address:
[a] Chemical Biology Laboratory, National Cancer Institute, National Institutes of Health, Frederick, MD, USA

#co-first authors
*co-corresponding authors: a.ciulli@dundee.ac.uk and slokey@ucsc.edu

Abstract:

Bifunctional PROTAC degraders belong to "beyond Rule of 5" chemical space, and criteria for predicting their drug-like properties are underdeveloped. PROTAC components are often combined via late-stage amide couplings, due to the reliability and robustness of amide bond formation. Amides, however, can give rise to low cellular permeability and poor ADME properties. We hypothesized that a bioisosteric replacement of an amide with a less polar ester could lead to improvements in both physicochemical properties and bioactivity. Using a library of model compounds, bearing either amides or esters at various linker-warhead junctions, we identify parameters for optimal compound lipophilicity and permeability. We next applied these learnings to design a set of novel amide-to-ester substituted, VHL-based BET degraders with increased permeability. Our ester-PROTACs remarkably retained intracellular stability, were overall more potent degraders than their amide counterparts and showed an earlier onset of the hook effect. These enhanced cellular features were found to be driven by greater cell permeability rather than improvements in ternary complex formation. This largely unexplored amide-to-ester substitution therefore provides a simple and practical strategy to enhance PROTAC permeability and degradation performance. Such approach could prove equally beneficial to other classes of beyond Ro5 molecules.

1 Introduction:

Targeted protein degraders, also known as Proteolysis Targeting Chimeras (PROTACs), are becoming a widespread source of chemical probes and lead compounds that degrade rather than inhibit target proteins, providing a different drug modality with potential to expand the "druggable" proteome.[1-7] These chimeric molecules typically contain a protein-of-interest (POI)-targeting ligand (or warhead) and a ligand which binds to an E3 ligase, connected by a linker.[8-10] PROTAC-induced ternary complexes between the POI and E3 ligase are required for polyubiquitination and targeted degradation of the POI.[11] PROTACs do not require full target occupancy, because a single PROTAC molecule can induce degradation of more than one target protein molecule over time, thereby acting catalytically at sub-stoichiometric target occupancy. These distinct features of PROTACs mode of action have been shown to result in increased target selectivity, higher potencies, and fewer off-target effects compared to small molecule inhibitors.[10, 12-14] Furthermore, unlike small molecule inhibitors, PROTACs can bind the target at any position, including non-functional binding sites.[10, 15] Notably, PROTACs have shown to be developable for use in humans, with several compounds reaching the clinic, including ARV-110 and ARV-471 that have recently progressed into Phase II clinical trials for prostate and breast cancer, respectively, demonstrating both safety and efficacy in patients.[16-18]

While PROTACs harbor several advantages as a new modality within drug discovery, their bifunctional nature and chemical composition mean that they are inherently larger than the warhead ligands on which they are based. This makes PROTAC compounds go beyond the "Rule of 5" (bRo5), and can impose hurdles to their pharmaceutical development.[19-22] Thus, efforts have been made recently to better understand the physicochemical properties and structure-property relationships of PROTACs in order to identify design parameters that may help guide development in this chemical space.[22-27] An important pharmacokinetic hurdle for high molecular weight compounds tends to be permeability.[28-29] Uptake into cells occurs in competition with efflux, which is also commonly a problem for large molecules.[30] Indeed, recently we and others have established that PROTACs can show potent cellular activity despite exhibiting very low permeabilities compared to their individual ligand components and to more conventional inhibitors.[31-33] There is therefore a great interest to develop strategies for improving cell permeability and other physicochemical properties of PROTACs.

We wondered whether PROTAC degradation activity could be improved by increasing their cell permeability. To this end, it is worth keeping in mind that requirements on cellular permeability are relaxed because, unlike inhibitors, PROTACs do not have to fully occupy the target binding site for the duration of their action. Indeed, the catalytic mode of action of PROTAC degraders via formation of stable ternary complex can compensate for low membrane permeability, as we have shown for the archetypical BET degrader MZ1.[31, 34] However, optimal ternary complexes are often challenging to achieve without the "trial and error" approach involving the synthesis and testing of many compounds.[35-36] Thus, we aimed to develop a set of simple parameters for optimization which could be applied during initial compound design or to existing PROTACs in order to improve bioactivity through increased membrane permeability.

In our previous work, we demonstrated that an amide-to-ester substitution at the *tert*-Leu of the von Hippel–Lindau (VHL)-recruiting ligand can increase membrane permeability.[31] While effective, this ester modification yielded only a modest increase in permeability over their amide counterparts due to the relatively high steric shielding at this position from the β-branched amino acid sidechain.[37] We hypothesized that alternatively, substituting the amide connecting the linker to the POI warhead for an ester would lead to a larger increase in permeability. Therefore, to build

on our proof-of-concept study, we developed a systematic set of compounds to test this hypothesis across a wide range of lipophilicities (ALogP) and linker lengths. By applying the insights from these model compounds, we show that the correct combination of an amide-to-ester substitution and ALogP modulation dramatically increased the membrane permeability of known bromodomain and extra terminal (BET) protein targeting PROTACs, MZ1 and ARV-771.[3, 38] These subtle structural modifications have also led to an increased ability to degrade BET proteins and induce cytotoxicity, while maintaining both stable ternary complex formation and plasma stability.

2 Results and Discussion:

2.1 Model-compound "liposcan" reveals ideal lipophilicity range for increased permeability

It is important to consider lipophilicity during compound design to attain molecules with favorable absorption, distribution, metabolism, excretion, and toxicity (ADMET) properties.[39] While suggested optimal lipophilicity ranges exist for typical small molecule drugs[40] and bRo5 compounds,[41] design parameters for ideal PROTAC lipophilicity remain unclear. We set out to perform a systematic investigation into the effect of lipophilicity on permeability for a set of seven VHL-based "PROTAC-like" model compounds (**1 – 7**, Figure 1). All compounds contained the VHL ligand VH032 as their E3 ligase-targeting ligand.[42] We modulated the compounds' lipophilicities using a variety of simple warheads as surrogates of POI ligands across a range of calculated lipophilicities (ALogP) from 1.2 – 6.0. As permeability can be strongly affected by molecular weight (MW) and the number of hydrogen bond donors (HBDs) and acceptors (HBAs), we kept these values in a relatively narrow range (MW = 600 – 800, HBD = 3 – 4, HBA = 6 – 8, SI Table 1). Furthermore, we used a short alkyl linker for compounds **1** – **7** to eliminate permeability-affecting intramolecular hydrogen bonds (IMHBs) that can be formed between polyethylene glycol (PEG)-based linkers and amide -NHs in other parts of the molecule.[25, 31]

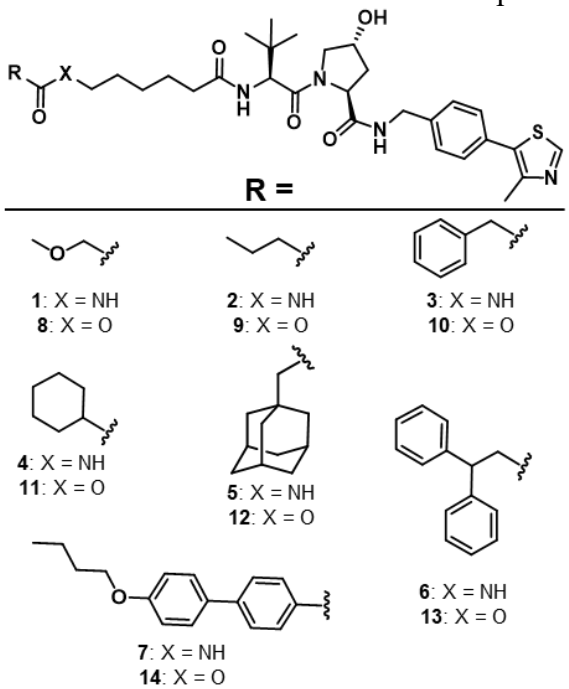

Figure 1: Liposcan model compound structures. Chemical structures of compounds organized by amide (**1 – 7**) and ester (**8 – 14**) matched pairs with warheads of varying lipophilicities

We next investigated the effects of lipophilicity on membrane permeability using the parallel artificial membrane permeability assay (PAMPA), a high-throughput permeability assay that is generally well correlated to cell-based permeability measurements.[43] Our group has shown that PAMPA is beneficial for studying compounds with low expected permeabilities due to the assay's low limit of detection.[31] Similar to other types of previously studied compounds,[41] the permeabilities of the model compounds increased with ALogP up to an ALogP of around 4 (cf. **1 – 5**, Figure 2A-B, SI Table 1). Above an ALogP of 4, permeability decreased as ALogP increased (cf. **6 – 7**) with no detectable permeability for **7**, which had an ALogP of 6.0 (Figure 2A, Table 1). At these higher ALogP values (>4 – 5), compounds begin to lose aqueous solubility and become membrane retained, both of which can reduce passive membrane permeability.[44] The data with this compound series suggests that PROTACs based on VH032 should be designed with an ALogP between 3 – 5 to bias them towards higher permeability, similar to other bRo5 compounds. Moreover, the relationship between lipophilicity and permeability offers a route to improve the permeability of PROTACs by making small structural modifications as needed to maintain ALogP within the optimal range.

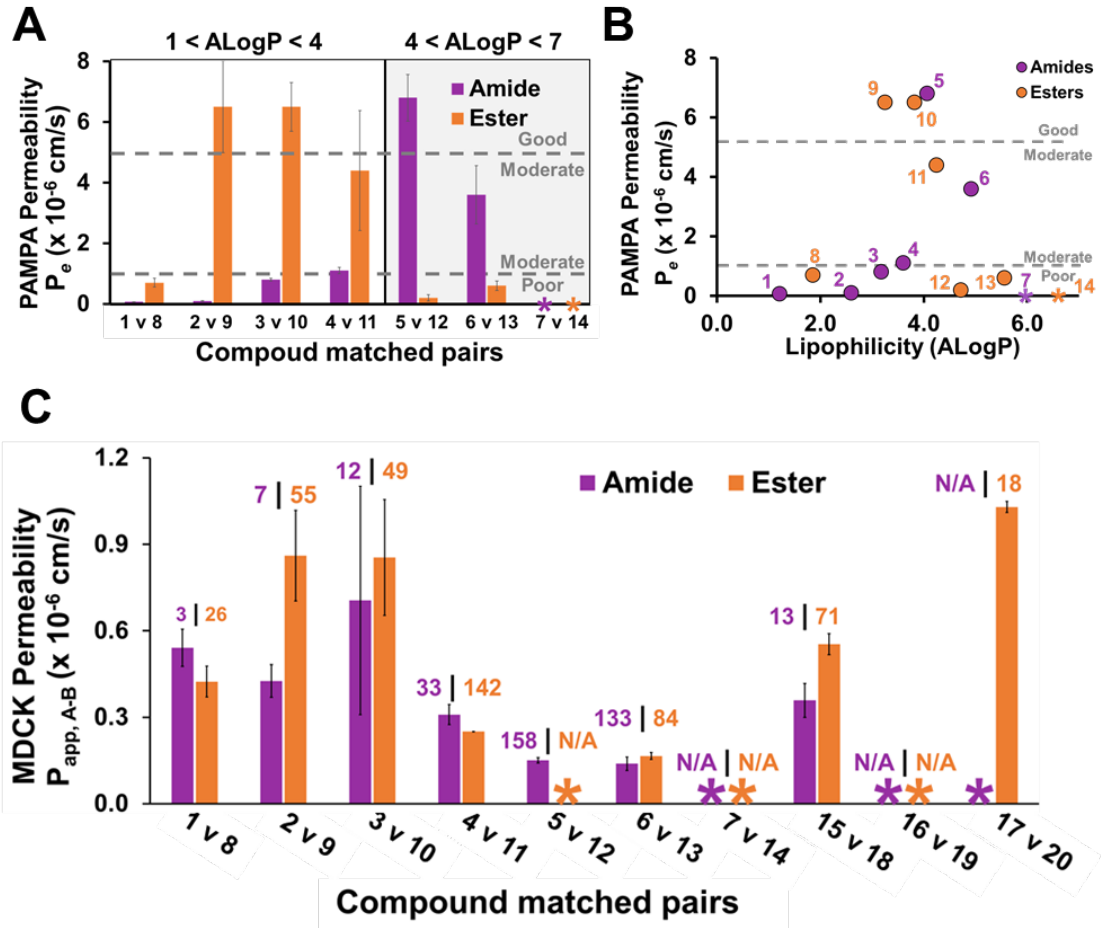

Figure 2: Liposcan model compounds permeabilities. PAMPA permeabilities of model compounds organized by (*A*) amide (purple) and ester (orange) matched pair (error bars represent ±SD, N=4) and (*B*) calculated lipophilicity (ALogP). Dashed grey lines represent categorical threshold for poor (P_e < 1 x 10^{-6} cm/s), moderate (1 x 10^{-6} cm/s < P_e < 5 x 10^{-6} cm/s), and good (P_e > 5 x 10^{-6} cm/s) membrane

permeability. (*C*) MDR1-MDCK cell permeability of liposcan and linker scan model compounds by matched pair. The numbers above bars indicate the efflux ratio. *below limit of detection, N/A: Efflux ratio could not be calculated. Error bars represent data range, N=2.

Table 1: Physicochemical and ADME properties of model compounds. Physicochemical properties including calculated lipophilicity (ALogP), experimental $LogD_{(dec/w)}$, calculated LP, and experimental plasma stability data of liposcan and linker scan model compounds for both amide and ester derivatives.

		Cmpd[a]	ALogP[b]	LogD (dec/w)[c]	LPE[d]	ΔLPE[e]	Plasma stability[f]
Liposcan	Amide	**1**	1.2	-2.2	2.0	*(see 8)*	126 ± 4%
		2	2.6	-2.2	0.5	*(see 9)*	83 ± 5%
		3	3.2	-1.5	0.6	*(see 10)*	130 ± 3%
		4	3.6	-1.4	0.3	*(see 11)*	168 ± 20%
		5	4.1	-0.2	1.0	*(see 12)*	74 ± 8%
		6	4.9	-0.3	-0.1	*(see 13)*	149 ± 9%
		7	6.0	1.0	0.1	*(see 14)*	83 ± 14%
	Ester	**8**	1.9	-1.7	1.8	-0.2	1 ± 0.4%
		9	3.2	-0.5	1.6	1.1	13 ± 1%
		10	3.8	0.8	2.3	1.6	57 ± 3%
		11	4.3	1.1	2.1	1.8	14 ± 1%
		12	4.7	2.4	2.8	1.8	80 ± 11%
		13	5.6	1.9	1.5	1.6	58 ± 6%
		14	6.6	BLD[g]	--	--	119 ± 28%
Linkers	Amide	**15**	1.8	-1.4	2.2	*(see 18)*	103 ± 14%
		16	1.7	-2.3	1.4	*(see 19)*	151 ± 30%
		17	1.6	-1.9	2.0	*(see 20)*	133 ± 18%
	Ester	**18**	2.5	-0.2	2.7	0.5	65 ± 28%
		19	2.3	-0.5	2.5	1.1	1 ± 0.1%
		20	2.2	-0.7	2.4	0.5	0.6 ± 0.1%

a: Compound
b: Calculated lipophilicity
c: 1,9-decadiene and PBS pH 7.4 shake flask partition coefficient
d: LPE = LogD(dec/w) – 1.06(ALogP) + 5.47
e: $\Delta LPE = LPE_{ester} - LPE_{amide}$, by amide-ester matched pairs, reference Figure 2C for full matched pair list
f: % compound remaining after 90 min in plasma at 37 ºC
g: Below limit of quantitation

Recently, it has been shown that PROTACs can have a high efflux ratio in cell-based permeability assays.[32-33] Therefore, we were interested in monitoring both the cell permeabilities and efflux ratios over this broad ALogP range. In bidirectional MDCK-MDR1 cells expressing human Pgp, amides **1** – **6** demonstrated generally low cell permeability, though these results were not strongly correlated to PAMPA or lipophilicity. As in PAMPA, **7** was below the limit of detection (Figure 2C, SI Table 2). Additionally, amides **1 – 6** also had high efflux ratios, suggesting

that they undergo active efflux.[45] Interestingly, these efflux ratios were highly correlated to both lipophilicity and PAMPA permeability. Efflux ratios increased with lipophilicity up to an ALogP of around 4, peaking with **5**. As with PAMPA permeability, the efflux ratio decreased with increasing lipophilicity at ALogP values above 4 (SI Tables 1 – 2).

2.2 Amide-to-ester substitutions improve membrane permeability over a broad ALogP range

In addition to lipophilicity, the number of HBDs in compounds is a crucial determinant of permeability.[46-47] Reducing the presence of solvent-exposed HBDs through N-methylation or occlusion from solvent by β-branching or other steric shielding are some of the strategies used to increase a compound's membrane permeability.[37, 48-50] In a previous study, we demonstrated that substituting the *tert*-Leu amide of the VH032 ligand with an ester improved compound permeability by about 2-fold.[31] We hypothesize that the relatively modest increase in permeability resulting from this amide-to-ester substitution was likely due to the partial shielding of the -NH from solvent by the adjacent β-branched α-carbon, limiting the permeability reducing effects of this HBD.[31, 37] Additionally, substituting this amide (between the VH032 ligand and the linker) for an ester reduced its binding affinity towards the VHL protein.[31] Therefore, we created a new set of compounds with an amide-to-ester substitution at the other end of the linker (adjacent to where a POI ligand would be attached) in an effort to achieve a more significant increase in permeability while maintaining binding to the VHL E3 ligase.

This second set of ester-containing, liposcan compounds (**8 – 14**) had a similarly broad ALogP range of 1.9 – 6.6 and narrow ranges for MW, HBAs, and HBDs (Figure 1, Table 1). These compounds were structurally identical to the previously described amides **1** – **7** except for an amide-to-ester substitution between the linker and the POI-ligand mimic, creating seven amide-to-ester matched pairs for permeability analysis. Over an ALogP range of 1 – 4, the esters, **8 – 14**, were 4- to 65-fold more permeable than their amide counterparts (Figure 2A, SI Table 1). Substituting an amide for an ester not only removes an HBD, but also increases the ALogP on average by about 0.6. Both the reduction of HBDs and increased lipophilicity are likely responsible for the increased permeability within this ALogP range.[37, 41, 51] However, as expected, esters with an ALogP > 4 were less permeable than their respective amide counterparts (Figure 2, SI Table 1). This is likely due to the inverse relationship between permeability and lipophilicity as the ALogP increases over 4 due to a decreased aqueous solubility and increased membrane retention of the compound.[52] Furthermore, it is possible that the additional HBD present in the amide series conferred increased solubility over the ester derivatives. Similar to amide **7** (ALogP = 6), its ester counterpart, **14**, (ALogP = 6.6) had no detectable permeability (Figure 2A, SI Table 1).

Notably, the esters achieved their peak permeability at a lower lipophilicity than the amides, at ALogP = 3.2 – 3.8 vs. ALogP = 4, respectively (Figure 2B). This ability to achieve higher membrane permeability at lower lipophilicities has important implications for drug development, as increased lipophilicity has been linked to increased toxicity and decreased specificity in addition to other liabilities associated with diminished solubility.[53] Though not as apparent as the PAMPA results, ester compounds had MDCK permeabilities that were also greater than or equal to their amide counterparts for the most part (Figure 2C). These MDCK cell and PAMPA permeabilities followed similar trends within the ester compound series, with **9** and **10** having the peak permeabilities in both assays (P_e = 6.5 x 10^{-6} cm/s, Figure 2, SI Table 1). These two ester compounds (**9** and **10**) also had very high efflux ratios in the MDCK assay compared to their amide counterparts (**2** and **3**, respectively). High efflux likely contributes to the diminished improvement in the MDCK cell permeabilities of the esters relative to the amides, compared to

those improvements observed in PAMPA. Much like the amide compounds, the ester series had a high efflux ratio that was similarly correlated to lipophilicity (SI Table 2). Overall, amide-to-ester substitution offers a highly effective strategy to improve PROTAC permeability over a wide range of lipophilicities.

2.3 Amide-to-ester substitutions increase permeability for several linker types

It has been suggested that short alkyl linkers may be better for PROTAC permeability, as they help minimize the already high topological polar surface area (TPSA) and the number of HBAs present.[32-33] However, this hypothesis has not been fully tested. We have previously shown that the effect of the linker on PROTAC permeability can be confounded by hydrogen bonding and overall lipophilicity.[31] For this study, we designed a systematic set of four compounds to assess the effects of linker length and composition on permeability by reducing the POI-ligand mimic to a simple benzyl group attached by an amide. The linkers varied from a short alkyl linker (**3**) to PEG-based linkers ranging from 1- to 3-PEG units in length (**15** – **17**, respectively) (Figure 3A, Table 1). The alkyl-linked compound **3** had the highest permeability. Permeability decreased with increasing PEG chain linker length with **17** (3-PEG unit linker) showing no detectable permeability (Figure 3B, SI Table 1). This decrease in permeability is likely caused by a decrease in ALogP due to the increasing PEG chain length, consistent with the linear relationship between ALogP and permeability in this lipophilicity range (Table 1).

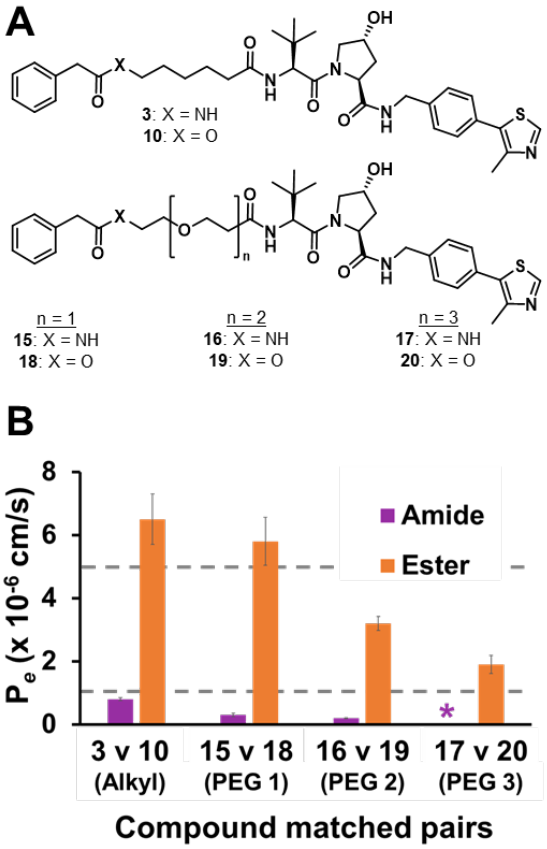

Figure 3: Linker scan model compound structures and permeabilities. (*A*) Chemical structures of linker scan model compounds (*B*) PAMPA permeabilities of model compounds organized by amide (purple) and ester (orange) matched pair. Dashed grey lines represent categorical threshold for poor (P_e < 1 x

10^{-6} cm/s), moderate (1 x 10^{-6} cm/s < P_e < 5 x 10^{-6} cm/s), and good (P_e > 5 x 10^{-6} cm/s) membrane permeability.

As an amide-to-ester substitution was found to improve the permeability of our first compound series of model compounds (**1** – **14**), we decided to make a second set of amide-to-ester compound matched pairs and synthesized esters **10**, **18** – **20** (Figure 3A). The esters all had detectable permeabilities that were 8- to 19-fold more permeable than their amide counterparts (Figure 3B, SI Table 1). Unlike the amides, which all had poor permeabilities (P_e < 1 x 10^{-6} cm/s), all the esters had modest to good permeabilities (1 x 10^{-6} cm/s < P_e < 5 x 10^{-6} cm/s). Thus, an amide-to-ester substitution improves permeability and offers more flexibility in compound design as a wider range of ester linkers are more likely to be permeable than their amide counterparts. This design flexibility is crucial since small modifications to the linker can significantly affect PROTAC bioactivity, ternary complex formation, and subsequent targeted degradation.[3, 54-55]

2.4 PROTACs exhibit ligand-to-linker intramolecular hydrogen bonds

The characteristic structure of PROTACs, two small molecules connected by a flexible linker, lends itself to the formation of intramolecular hydrogen bonds (IMHBs). This important feature allows for polar atoms to be shuttled across the lipophilic cell membrane. It is difficult to determine the presence of IMHBs by inspecting the 2D chemical structure alone. However, measuring the lipophilic permeability efficiency (LPE) of matched pairs can indicate differences in the number of exposed HBDs.[31, 41] LPE is a metric that balances aqueous solubility (calculated ALogP) and membrane partitioning (experimental $LogD_{(dec/w)}$) to determine the efficiency with which a compound crosses a membrane at a given lipophilicity. Similar to the previously developed ΔLogP metric,[47, 56-58] LPE is particularly valuable in determining differences in solvent-exposed HBDs between compounds. Compounds with similar LPE values are likely to have the same number of solvent-exposed HBDs, while a ΔLPE of 1.8 suggests the difference of a single exposed HBD (compounds with higher LPE values have fewer exposed HBDs).[41]

For the majority of the liposcan compound pairs (**2** – **6** vs. **9 – 13**, respectively), the ester compounds had higher LPEs than their counterpart amide compounds (Table 1). The ΔLPEs of between 1.1 and 1.8 suggest that the additional HBD in the amide compounds is partially to fully solvent-exposed. Interestingly, the amide compounds with an ether oxygen five atoms away from the amide -NH had similarly low ΔLPEs (cf. **1** vs. **8**, **15** vs. **18**, and **17** vs. **20**, Table 1). Consistent with previous work,[31, 59-60] this suggests that the amide -NH is making an IMHB with the ether oxygen in the PEG linker (**15** and **17**) or the OMe ether oxygen of a POI ligand mimic (**1**). These results are also consistent with recent work from Kihlberg, et al., who used NMR to show IMHB between PROTAC warheads and the oxygen atoms in their PEG linkers.[25] Therefore, while ester bonds and alkyl linkers are better for permeability, when used in combination, a PEG linker and amide bond could be used to shield the polarity of important HBDs that are crucial to the bioactivity or solubility of the overall molecule.

2.5 Esters maintain plasma stability and binding to the VHL E3 ligase

While amide-to-ester substitutions offer increased permeability, leading to increased flexibility in compound design, esters are also typically more susceptible to plasma-mediated hydrolysis, which can lead to low *in vivo* efficacy.[61] For these amide-to-ester substitutions to be a viable option in drug development, it is crucial to compare the stability of ester and amide compounds. We incubated **1** – **20** in human plasma at 37 ºC for 0, 15, 30, and 90 min to test this.

Overall, the amides were more stable in plasma than their ester counterparts. This effect was more pronounced for compound pairs with smaller, sterically unhindered POI-ligand mimics, with ≤10% compound loss of the amide compounds at 90 min (**1 – 4**) compared to 60 – 90% compound loss at 90 min for their ester counterparts (**8 – 11**) (Table 1, SI Figure 1). Esters **12 – 14** contained larger warheads with likely more steric shielding around the susceptible ester. These compounds had much lower compound loss after 90 min (4 – 10%, Table 1, SI Figure 1). This reduced hydrolysis, evident with bulky substituents, suggests that amide-to-ester substitutions could be used to increase PROTAC permeability without affecting PROTAC *in vivo* or *in cellulo* activity as these larger substituents more closely represent typical POI ligands present in PROTACs.

Maintaining target binding affinity is another crucial feature to consider while optimizing PROTACs for improved permeability. As previously mentioned, an amide-to-ester substitution between the linker and the VHL-ligand decreased binding affinity by about 2-fold.[31] In this work, we used a similar fluorescence polarization (FP) competition binding assay to determine if the amide-to-ester substitution between the linker and the POI-ligand mimic, was more tolerated when binding to the VHL protein. Using our second amide (**3**, **15** – **17**) and ester (**10**, **18** – **20**) series, comprised of varying linker lengths, we found that both amides and esters had FP-derived dissociation constants (K_d) that were broadly comparable to each other at each linker length (SI Figure 2). The amides appeared to show slightly better binding at each linker length compared with their ester counterparts, yet the K_d values were roughly within the error of each pair. Interestingly, changes in linker length had a more pronounced effect on VHL-binding than the amide-to-ester modification. The two compounds with alkyl linkers, **3** and **10**, had K_d values (119 nM and 136 nM, respectively) more similar to VH032 alone (113 nM). Binding affinity was slightly reduced for all compounds containing PEG-based linkers, with 1-PEG and 2-PEG units (amides **15 – 16** $K_d \approx$ 170 nM and esters **18 – 19** $K_d \approx$ 200 nM, respectively) showing comparable binding affinity. The longer 3-PEG unit compounds (**17** and **20**) showed slight recovery, with K_d values (138 nM and 144 nM, respectively) closer to their alkyl chain counterparts **3** and **10** (119 nM and 136 nM, respectively) for both amide and ester compounds (SI Figure 2). However, the K_d values for all compounds in this linker series (either amide or ester) were within 2-fold of the VH032 ligand alone. Encouragingly, this suggests that, for a given linker, an amide-to-ester substitution away from the E3 ligand will have little to no effect on E3 binary binding.

2.6 Applying model compound findings to a PROTAC library

With this model-toolkit for improving PROTAC permeability in hand, we were curious to determine if we could apply these insights to improve PROTAC permeability and, as a result, their degradation activity. To test this idea, we decided to study two previously published and structurally similar BET-targeting PROTACs, MZ1 (**21**)[3] and ARV-771 (**22**).[38] MZ1 is comprised of a pan-selective triazolothienodiazepine BET inhibitor, (+)-JQ1,[62] connected to the VHL-ligand VH032 via a 3-PEG-based linker. ARV-771 uses the same BET-targeting ligand, but differs from MZ1 by having a slightly shorter, more lipophilic linker (minus CH_2-O), and containing an extra chiral methyl group at the benzyl position of the VHL ligand. Because both esters and amides at the linkage point of JQ1 are equally effective at binding to BET bromodomains,[63-65] we reasoned MZ1 and ARV-771 would provide an ideal model system to study the effect of the amide-to-ester substitution without interfering with binary POI binding affinity. Using a combination of amide-to-ester substitutions between JQ1 and the linker, and subtle modifications to linker length and composition, we designed and synthesized compounds **23** – **28** (Table 2) with a goal to improve the degrader activity through increased permeability.

Table 2: PROTAC toolbox. Chemical structures, calculated lipophilicity (AlogP) and PAMPA permeabilities for **21 – 28** including existing BET degraders, MZ1 (**21**) and ARV-771 (**22**). For detailed synthetic procedures, see the Supporting Information. *PAMPA P_e values are $\times 10^{-6}$ cm/s.

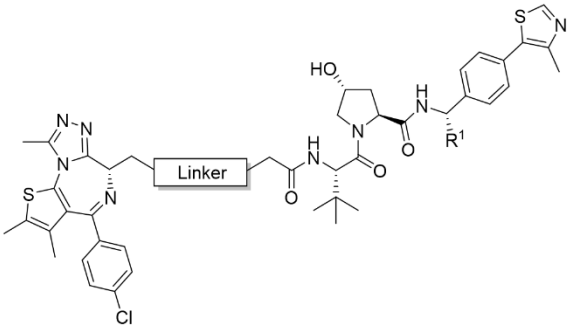

Cmpd	Linker	R¹	ALog P	PAMPA*	Cmpd	Linker	R¹	ALog P	PAMPA*
21	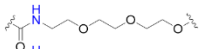	H	3.6	0.01	**25**	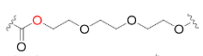	H	4.3	0.1
22	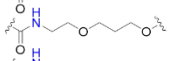	Me	4.2	0.2	**26**	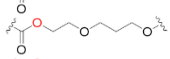	Me	4.8	0.3
23	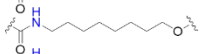	H	4.8	0.5	**27**	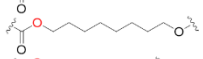	H	5.5	0.2
24	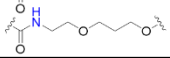	H	3.8	0.08	**28**	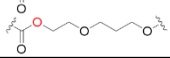	H	4.4	0.6

2.7 Improving PROTAC permeability increases PROTAC bioactivity

Overall, the PAMPA permeabilities of our new PROTAC series followed the same trends shown by our model compounds. In three of the four amide-to-ester matched pairs (MZ1 (**21**) and OMZ1 (**25**), ARV-771 (**22**) and OARV-771 (**26**), and AB2 (**24**) and OAB2 (**28**)), the amide-to-ester substitution led to an increase in permeability by 10-, 1.5- and 7.5-fold, respectively (Table 2, Figure 4A, SI Table 3). As expected, substituting the amide in AB1 (**23**) for an ester in OAB1 (**27**) caused a 2.5-fold reduction in permeability in the last matched pair. This decrease in permeability is due to the increased lipophilicity of **27**, ALogP = 5.5, pushing the ester into the insoluble ALogP regime. Compound **28** had the highest PAMPA permeability (0.6 x 10^{-6} cm/s), with an ALogP of 4.4. PROTACs with ALogP values >4.4 started to show a decrease in PAMPA permeability (Figure 4A). Compounds **22** and **26** contained an extra chiral methyl group at the benzyl position of the VH032 ligand. The effects of this additional methyl group on permeability can be seen when comparing two alternative matched pairs within the amide series, **22** vs **24**, and within the ester series, **26** vs **28**. In the amide pairing, an additional methyl group increases PAMPA permeability by 2.5-fold, whereas, in the case of the ester pairing, permeability decreases by 2-fold. Again, these trends are likely the result of the "inverted-parabola" relationship between ALogP and permeability.[66-68] As MDCK permeability measurements are less sensitive to poor compound solubility than PAMPA permeability at high lipophilicities,[41, 66] we attempted to collect MDCK cell permeabilities for these PROTAC compounds starting with **21** and **25**. However, both compounds were below the limit of detection in the apical to basal permeation (SI Table 2). Thus, we did not pursue MDCK permeabilities on the remaining PROTACs. Taken together, our data are consistent with increasing lipophilicity and reducing PEG-like character of the PROTAC linker, producing similar trends in permeability as described for the model compounds above. Furthermore, all eight PROTACs were stable in plasma after 90 minutes with no detectable reduction in PROTAC levels (Figure 4B). This suggests that a rigid and sterically bulky POI-

ligand, like JQ1, provides sufficient protection from ester hydrolysis, as also suggested by the model compounds.

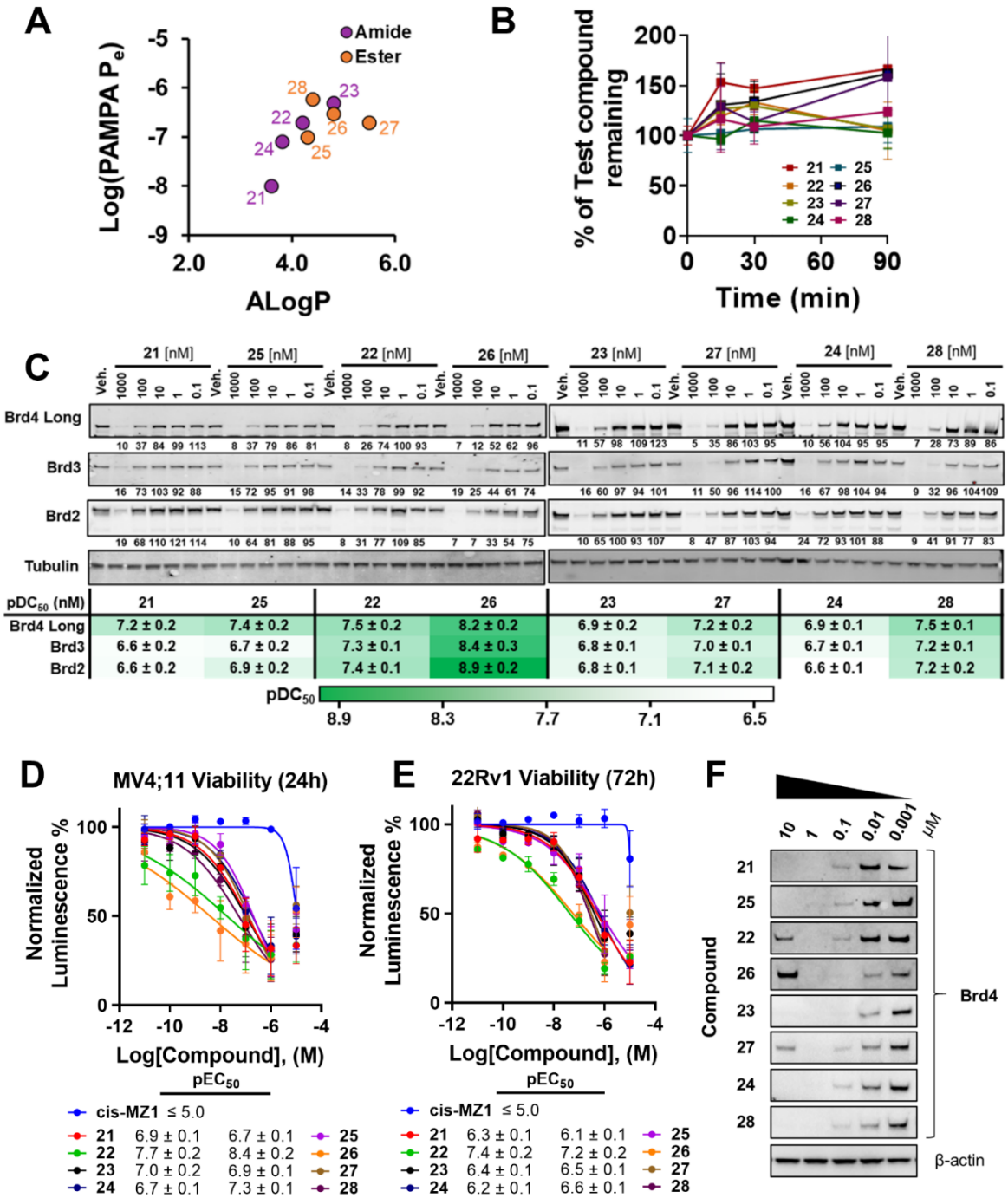

Figure 4: PROTAC permeability, stability and cellular activity. (*A*) Permeabilities of PROTACs **21** – **28** compared with calculated lipophilicity (ALogP); (*B*) Percent of PROTAC remaining after 0, 10, 30, and 90 min in plasma at 37 ºC, normalized to the 0 min time point; Cellular activity of PROTACs **21** – **28**. (*C*) Western blot data for BET protein levels monitored from 1 μM to 100 pM compound treatment over 4 h in HEK293 cells. Bands were normalized to vehicle

control (DMSO) and tubulin. pDC_{50} values (± S.E.M) are mean from 3 independent experiments. (D), (E) Antiproliferation of PROTACs **21** – **28** and non-degrader control cis-MZ1. MV4;11 (D) and 22Rv1 (E) cells were treated with varying concentrations of compound, and after 24 and 72 h respectively, were subject to CellTiter-Glo cell viability assay. pEC_{50} values (± S.E.M) are mean from $N = 3$ for MV4;11 and $N = 2$ for 22Rv1. (F) Hook effect shown from western blot data for Brd4 protein levels monitored from 10 μM to 1 nM compound treatment over 4 h in HEK293 cells.

Next, we evaluated the cellular activities of all eight PROTACs in HEK293 cells to obtain a degradation (DC_{50}) profile for BET proteins, Brd4, Brd3, and Brd2 (Figure 4C, SI Figure 3 – 4). Notably, the improvements in permeability seen when substituting the amide in the known degraders **21** and **22** for an ester in **25** and **26** translated into meaningful improvements in bioactivity. Compound **25** showed a 1.5- to 2-fold increase in degradation potency over **21** for both Brd4 (DC_{50} = 44 nM vs 60 nM, respectively) and Brd2 (DC_{50} = 133 nM vs 230 nM, respectively), while **25** showed near equipotent degradation compared to **21** for Brd3 (DC_{50} = 221 nM vs 239 nM respectively). Strikingly, **26** showed to be the most potent degrader out of this series, with a 5.5-fold more potent degradation of Brd4 compared to its amide counterpart, **22** (DC_{50} = 6 nM vs 33 nM, respectively), a 42-fold increase for Brd2 (DC_{50} = 1 nM vs 42 nM, respectively) and a 12-fold increase for Brd3 (DC_{50} = 4 nM vs 47 nM, respectively). Similarly, **27** gave a 2-fold increase in degradation potency over its amide counterpart, **23** for both Brd4 (DC_{50} = 133 nM vs 57 nM, respectively) and Brd2 (DC_{50} = 87 nM vs 166 nM, respectively), and also, a 1.5-fold increase with Brd3 (DC_{50} = 107 nM vs 158 nM, respectively). Finally, **28** showed a 4-fold increase in degradation potency against Brd4 when compared to its amide counterpart, **24** (DC_{50} 31 nM vs 125 nM, respectively), a 4-fold increase with Brd2 (DC_{50} = 68 nM vs 273 nM, respectively) and a 3.2-fold increase with Brd3 (DC_{50} = 68 nM vs 273 nM, respectively) (Figure 4C, SI Figure 4). Together, the cellular degradation data demonstrate that the amide-to-ester substitution has a profound beneficial effect on PROTAC activity.

We and others have shown that improved PROTAC-induced degradation of BET protein translates to enhanced effect in the viability of BET-dependent cancer cell lines.[38, 69] We therefore moved to evaluate the cytotoxicity of our PROTAC series by assessing the viability of BET-sensitive lines MV4;11 (acute myeloid leukemia) (Figure 4D) and 22Rv1 (human prostate carcinoma) (Figure 4E). All PROTACs exhibited a marked antiproliferative effect on each cell line, consistent with their activity as degraders. Compounds **22** and **26** gave the most pronounced effect with EC_{50} values of 18 nM and 4 nM in MV4;11, respectively, and 44 nM and 58 nM in 22Rv1, respectively. Notably, out of the non-methylated VH032-based PROTACs, **28** was the most effective with EC_{50} values of 53 nM and 250 nM for MV4;11 and 22Rv1, respectively. This compound had the highest PAMPA permeability ($P_e = 0.6 \times 10^{-6}$ cm/s, Table 2, SI Table 3) suggesting that it permeates membranes more effectively and is thus able to start the catalytic cycle of ternary complex formation, ubiquitination, and degradation at lower compound dose, leading to increased cell antiproliferation. Furthermore, it is because of this catalytic activity at sub-stoichiometric concentration that even a modest improvement in permeability can significantly increase a PROTAC's degradation activity and cytotoxicity.

Interestingly, in MV4;11 cells, all of the PROTACs became less effective at higher concentrations (10 μM) (Figure 4D). This was ascribed to be due to the "hook-effect",[70] a well-known phenomenon with bifunctional PROTAC degraders, where at high concentrations,

unproductive binary complexes of PROTAC:E3 ligase and of PROTAC:POI outcompete ternary complex formation (POI:PROTAC:E3 ligase). Moreover, in 22Rv1 cells, all PROTACs, with the exceptions of **21**, **24** and **25,** exhibited a hook effect to varying degrees (Figure 4E). Interestingly, **22**, **23**, **26**, **27** and **28** all have PAMPA permeabilities $\geq 0.2 \times 10^{-6}$ cm/s and generally higher ALogP values than **21**, **24** and **25**. This suggests that **22**, **23**, **26**, **27** and **28** likely enter the cell more efficiently, leading to higher intracellular PROTAC concentrations, and thus more pronounced hook effects. On broader terms, this correlation between PAMPA permeabilities and the hook effect further supports that the PAMPA permeabilities measured with our PROTAC set translate into relevant trends in their cellular activity profiles.

To further evaluate the observed hook effect seen in the cell viability assay, we decided to orthogonally investigate this in cell degradation assays by western blot, assessing Brd4 protein levels in HEK293 cells starting with a 10 μM treatment of PROTAC (Figure 4F). Strikingly, ester compounds **26** and **27**, and also amide **22**, exhibited a hook effect at 10 μM. Compounds **22** and **26** both possess an extra methyl on the VH032 ligand, which enhances binary binding affinity to VHL. A possible explanation for the observed onset of the hook effect in **22** and **26** is that their stronger binding to VHL contributes to the binary complex being more effective at outcompeting the ternary complex formation. Alternatively, this could also be attributed to the increased lipophilicity and permeability conferred by the added methyl group (cf. **22** vs **24** and **26** vs **28**, Table 2, SI Table 3). Similarly, **26** appears to hook to a greater extent than its amide counterpart **22**, suggesting that intracellular concentrations of **26** are higher, most likely due to the increase in lipophilicity and PAMPA permeability (cf. Table 2, Figure 4A, SI Table 3). Interestingly, **27** is the only non-methylated VH032-based compound that exhibited the hook effect. This could be due to **27** being the most lipophilic compound out of the series (ALogP = 5.5).

2.8 Improved potency is due to improved permeability rather than improvements to ternary complex formation.

We have previously shown that the PROTAC MZ1 forms highly cooperative, stable, and long-lived ternary complexes with BET bromodomains, with preference for BD2s over BD1s, and in particular for $Brd4^{BD2}$, and that these biophysical characteristics of the ternary complex underpin a high level of target ubiquitination and drive potent and fast degradation activity of MZ1 with Brd4.[34, 59, 71] We thus wondered to what extent the improvements in cellular activity that we observed with our set of PROTACs might be contributed from more favorable ternary complex formation. To address this question, we biophysically characterized all compounds in our PROTAC series by measuring both binary binding to VHL and ternary complex formation between VHL, PROTAC, and both BD1 and BD2 bromodomains of Brd4, Brd3 and Brd2 (Figure 5, SI Table 4). We measured cooperativity across the entire set of eight PROTACs vs six bromodomains (48 combinations). We used a competitive FP assay in which a fluorescently labelled HIF-1α peptide probe bound to VHL is displaced by titrating either PROTAC alone (for binary binding) or by titrating PROTACs preincubated with individual BET bromodomains (for ternary complex binding). This allows us to calculate the cooperativity (α) of ternary complex formation ($\alpha = K_d^{binary} / K_d^{ternary}$, Figure 5C).[34, 59, 69, 72-73]

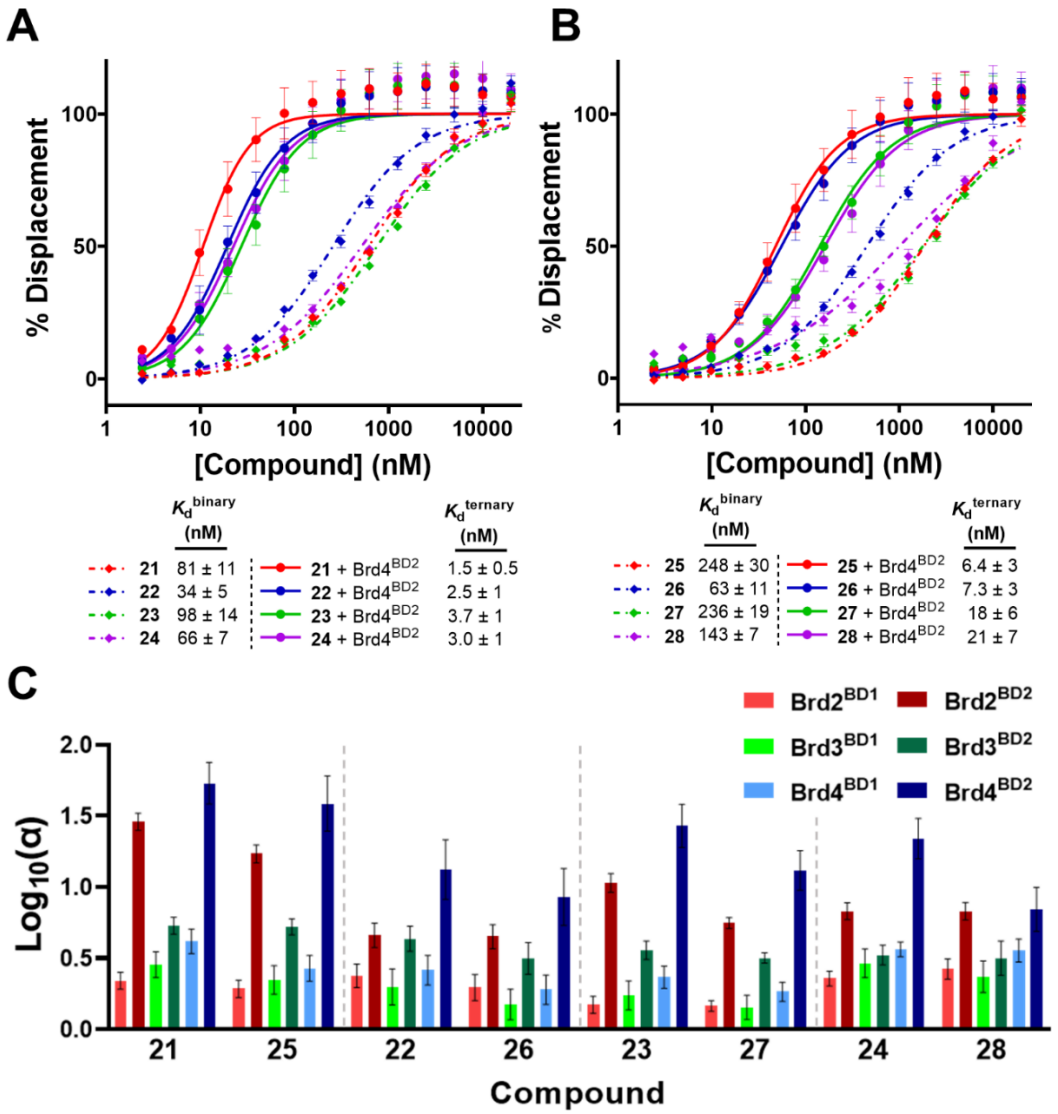

Figure 5: Fluorescence polarization (FP) of PROTAC binding. Binary and ternary complex formation FP data for amide (*A*) and ester (*B*) PROTACs to VHL alone (diamonds and dashed line) or preincubated Brd4^{BD2} with PROTAC to VHL (circles and solid line). K_d values are mean ± SEM from $N = 5 – 6$ for binary binding to VHL and $N = 3$ for ternary binding. Left-shift between binary and ternary data indicates positive cooperativity. FP binding data for the remaining five BET proteins can be found in the supplementary information. (C) Cooperativity (α) is plotted as $Log_{10}(α)$ (± propagated uncertainty). Grey dashed lines separate amide-to-ester matched pairs.

Strikingly, in all amide-to-ester matched pairs, the esters were 2 to 3-fold weaker at binding to VHL, with the largest difference being between **21** (K_d = 81 nM) and **25** (K_d = 248 nM). As expected, due to the additional benzyl methyl group present in the VH032 ligand,[74] PROTACs **22** and **26** showed the strongest binary binding to VHL (K_d = 34 nM and 63 nM, respectively). Additionally, all esters were also 2- to 7-fold weaker than their amide counterparts at binding VHL

when pre-bound to each individual BET bromodomain, as measured by their ternary K_d values (cf. Fig. 6B vs 6A). One hypothesis for this decreased binding affinity is the formation of a new IMHB between the new HBA present in the ester group and a HBD of an amide in the VH032 ligand. This could cause the rigid and relatively bulky JQ1 ligand to sit on top of the VHL protein, potentially causing unfavorable clashes and requiring an energetic penalty to allow binding to VHL. This is somewhat evident when switching from a PEG linker in **25** to a more alkyl linker in and **27** which has negligible effects on VHL binding; however, shortening the linker in **28** gave a 1.75-fold increase in affinity. The shorter linker decreases flexibility for the molecule to fold and form new IMHBs. Recently, others have shown how VHL targeting PROTACs can fold and form IMHBs in different solutions to change their TPSA.[25] Further structural studies are warranted to fully assess this phenomenon in the PROTACs presented here.

In all cases, PROTACs formed preferential and more positively cooperative ternary complexes with the second bromodomain (BD2) of each BET protein over the first bromodomain (BD1), consistent with what is observed with MZ1 (see refs.[34, 59] and data herein, cf. **21**). All PROTACs displayed cooperative ternary complexes with all BET BDs ($\alpha > 1$, Figure 5C, SI Table 4). Interestingly, all esters, albeit retaining positive cooperativity with each BET BD, were slightly less cooperative than their amide counterparts. Ternary complexes between $Brd4^{BD2}$, PROTAC, and VHL formed the strongest and most cooperative ternary complex, as in the case of MZ1 (**21**).[14, 34] This can be seen by a left-shift in the FP displacement curve when the bromodomain is present (Figure 5A-B). Interestingly, **21**, **25**, **23** and **27**, which all have the same linker length, follow the same intra-BET bromodomain cooperativity profile (Figure 5C), suggesting that these compounds form similar ternary complexes to one another. In contrast, compounds **22**, **26**, **24** and **28**, which all contain the same, shorter linker, were found to be less discriminatory between individual bromodomains. Based on these results we conclude that these four compounds likely form ternary complexes that, while similar to one another, are significantly different from the structurally-resolved complex of MZ1 (**21**).[59] Importantly, within these sets of compounds with the same linker length, each amide-to-ester matched pair showed identical intra-BET selectivity profile, strongly suggesting that each pair forms highly similar ternary complex.

Noticeably, MZ1 (**21**) formed the strongest $Brd4^{BD2}$:PROTAC:VHL complex ($K_d^{ternary}$ = 1.5 nM, $\alpha = 54$), values comparable to earlier work by Roy et al. ($\alpha = 55$),[34] with **28** forming the weakest ($K_d^{ternary}$ = 21 nM, $\alpha = 7$) out of the series. When comparing MZ1 (**21**) and ARV-771 (**22**), **22** showed near equipotent ternary binding to **21** ($K_d^{ternary}$ = 2.5 nM). However, the complex induced by **22** was 4-fold less cooperative ($\alpha = 13$) than the complex induced by **21** ($\alpha = 54$). Despite this reduced cooperativity, **22** was a more potent degrader across all three BET domains and was more cytotoxic in both cell lines than **21** (Figure 4C-E). However, due to the expected differences in ternary complexes formed by **22** and **21**, it is difficult to dissect whether the major factor in the improved cellular activity of **22** over **21** is a 2-fold higher VHL binding affinity (K_d^{binary} = 34 nM and 81 nM, respectively) or the 20-fold increase in membrane permeability of **22** over **21** (P_e = 0.2 x 10-6 cm/s and 0.01 x 10-6 cm/s, respectively, Table 2 and SI Table 3). Either way, this does suggest that some combination of increased VHL binding and membrane permeability can compensate for reduced cooperativity, albeit at the expense of an earlier onset of the hook effect.

The similar biophysical profiles of the amide-ester matched pairs allow more robust assessment of the contribution of cell permeability to PROTAC degradation activity for these compounds. Analysis of these matched pairs makes it clear that increased protein degradation for these compounds must be driven by increased cell permeability rather than ternary complex

formation. For example, the ester matched pair of MZ1 (cf. **25** and **21**), **25**, was found to be 1.5-fold more potent than **21** at degrading Brd4 (Figure 4C), despite **25** having 3-fold weaker binary and ternary affinities to VHL ± $Brd4^{BD2}$ than **21** and also forming a less cooperative complex (α = 39 vs 54, respectively). Therefore, it is evident that the increased potency is derived from the 10-fold increase in membrane permeability of **25** compared to **21** (Figures 4-5). Similarly, the ester matched pair of ARV-771 (cf. **26** and **22**), **26**, displayed a 5.5-fold increase in Brd4 degradation potency relative to **22**, despite having 2- to 3-fold weaker binary and ternary affinities to VHL ± $Brd4^{BD2}$ than **22**, and also forming a less cooperative ternary complex (α = 8.5 vs 13, respectively). Finally, ester **28**, not only has the highest PAMPA permeability ($P_e = 0.6 \times 10^{-6}$ cm/s) of the entire PROTAC series and is 7.5-fold more permeable than its amide counterpart, **24**, but **28** also displays the most potent degradation of Brd4 in cells when compared with the other VH032-based PROTACs within the series (**21**, **25**, **23**, **27** and **24**). This is despite **28** having the lowest ternary affinity and cooperativity with $Brd4^{BD2}$ ($K_d^{ternary}$ = 21 nM, α = 7).

These observations suggest that protein degradation with these compounds must be driven by cell permeability rather than ternary complex formation. Indeed, for each matched pair, the ester is more permeable than the parent amide: **25** is more lipophilic and 10-fold more permeable than **21**; **26** is more lipophilic and 1.5-fold more permeable than **22**; and **28** has the highest PAMPA permeability ($P_e = 0.6 \times 10^{-6}$ cm/s) of the entire PROTAC series and is 7.5-fold more permeable than **24** (Table 2, Figure 4A, SI Table 3). These results also highlight the utility of PAMPA to ascertain biologically meaningful permeability differences among PROTACs, even among compounds whose absolute permeabilities are very low ($<10^{-6}$ cm/s). Taking these data altogether, it is evident that the greater activity of ester PROTACs relative to their amide counterparts is being influenced by their ability to permeate into cells more efficiently, thus, initiating the ternary complex-driven catalytic knock-down of target BET proteins at overall lower dose, resulting in more potent degrader compounds.

3 Conclusion

Composed of two binders and a linker, bifunctional PROTAC degraders typically fall in bRo5 space.[26] Chemists have recently been pushed to shift away from designing molecules in the traditional Ro5 chemical space [46, 75] as more bRo5 compounds are shown to be cell active, and developable in vivo, including being orally bioavailable.[28, 30] However, having general guidelines for physicochemical design parameters for bRo5 compounds like PROTACs is critical to improve their chances to be useful cellular probes and to be developable as drugs.[53] In response to this pressing need, some have attempted to improve permeability, solubility, and efflux ratios through linker modifications.[73] In contrast, others have also attempted to reduce the number of amide bonds (HBDs) to improve the physicochemical properties of PROTACs.[76] We and others have attempted to develop systematic studies of PROTAC physicochemical properties and new methods to study these properties.[22, 25, 31-33]

In this study, we have shown that PAMPA is a reliable predictor of PROTAC permeability that translates relatively well into their cellular activity profiles. This has allowed us to develop strategies of improving PROTAC potency by improving permeability despite the previously suggested propensity of PROTACs to actively undergo efflux. We used a systematic investigation of linker lengths and lipophilicity combined with amide-to-ester substitutions to improve the permeability of "PROTAC-like" model compounds. We demonstrated that the PROTACs studied herein achieve the highest permeability at moderate lipophilicities (3 – 5) and that, within this range, increasing the lipophilicity of a compound leads to increased permeability, as has been seen

with other beyond Ro5 compounds.[41] Designing compounds in this range (which we have found to contain more permeable compounds) is also likely to reduce toxicity.[53] We also demonstrate that amide-to-ester substitutions can increase PROTAC permeability in this ALogP range as well. Therefore, ester-containing compounds in this lipophilicity range are likely to have better overall pharmacokinetic properties than amide compounds or those with higher lipophilicities. Finally, though esters are more prone to hydrolysis and therefore tend to be less stable in plasma, we discovered that adding steric bulk to the chemical space surrounding the area (i.e., near the warhead) drastically reduces compound degradation in the plasma. Therefore, amide-to-ester substitutions remain a viable option for PROTAC pharmacokinetic improvement, leading to more compound reaching its intracellular target. In each amide-to-ester PROTAC matched pair, we have demonstrated that this simple functional group conversion can lead to significant increases in PROTAC bioactivity, despite esters showing weaker binding affinity than their amide counterparts. We therefore provide what are, to our knowledge, unprecedented examples of optimizing PROTAC degradation activity through systematic rational improvements in compound cell permeability. It is clear that the increase in lipophilicity and permeability shown by the esters and linker modified compounds relative to amides has a positive effect on cellular activity and should be considered when designing future degraders, while attempting to retain favorable productive ternary complex formation. Amide-to-esters substitution thus provide a simple and convenient bioisosteric replacement that we anticipate will find wide utility as an attractive strategy for development and optimization of PROTACs, as well as other emerging beyond Ro5 compounds of chemically-induced proximity.[77-79]

Acknowledgements:
We would like to thank Chad E. Townsend for his design of the in-house python program used to process mass spectrometry-based assay data. We would also like to thank Yi Sun for her assistance with synthesis and purification of compounds. Finally, we would also like to thank Dr. David Zollman for his assistance with the FP binding assays.

Notes:
The authors declare the following competing financial interest(s): The A.C. laboratory receives or has received sponsored research support from Almirall, Boehringer Ingelheim, Eisai Co., Nurix, Ono Pharmaceuticals, and Amphista Therapeutics. A.C. is a scientific founder, shareholder and consultant of Amphista Therapeutics, a company that is developing targeted protein degradation therapeutic platforms.

Author contributions:
The manuscript was created through contributions of all authors and edited by all. V.G.K. and A.G.B. contributed equally.

Funding sources:
Research reported in this publication was supported by the National Institute of General Medicine Studies of the National Institutes of Health under award number R01GM131135 (to R.S.L.), and by the Innovative Medicines Initiative 2 (IMI2) Joint Undertaking under grant agreement No 875510 (EUbOPEN project) from the European Union's Horizon 2020 research and innovation programme (to A.C.). V.G.K is funded by the National Science Foundation Graduate Research Fellowship Program (NSF DGE 1339067). A.G.B. is funded by a PhD studentship from the

Medical Research Scotland (MRS) (1170-2017). C.C. is funded by a PhD studentship from the UK Medical Research Council (MRC) under the doctoral training programme in Quantitative and Inter-disciplinary approaches to biomedical science (QI Biomed) (MR/N0123735/1). Biophysics and drug discovery activities at Dundee were supported by Wellcome Trust strategic awards 100476/Z/12/Z and 094090/Z/10/Z, respectively. Any opinions, findings, and conclusions or recommendations expressed in this material are those of the authors and do not necessarily reflect the views of the National Institutes of Health or the National Science Foundation.

Orcid ID:

Victoria G. Klein: 0000-0002-3438-2399
Adam G. Bond: 0000-0002-1271-1032
Conner Craigon: 0000-0001-8649-6876
R. Scott Lokey: 0000-0001-9891-1248
Alessio Ciulli: 0000-0002-8654-1670

References:

1. Lu, J.; Qian, Y.; Altieri, M.; Dong, H.; Wang, J.; Raina, K.; Hines, J.; Winkler, James D.; Crew, Andrew P.; Coleman, K.; Crews, Craig M., Hijacking the E3 Ubiquitin Ligase Cereblon to Efficiently Target BRD4. *Chem Biol.* **2015,** *22* (6), 755-763.
2. Winter, G. E.; Buckley, D. L.; Paulk, J.; Roberts, J. M.; Souza, A.; Dhe-Paganon, S.; Bradner, J. E., Phthalimide conjugation as a strategy for in vivo target protein degradation. *Science* **2015,** *348* (6241), 1376.
3. Zengerle, M.; Chan, K.-H.; Ciulli, A., Selective Small Molecule Induced Degradation of the BET Bromodomain Protein BRD4. *ACS Chem Biol.* **2015,** *10* (8), 1770-1777.
4. Chan, K.-H.; Zengerle, M.; Testa, A.; Ciulli, A., Impact of Target Warhead and Linkage Vector on Inducing Protein Degradation: Comparison of Bromodomain and Extra-Terminal (BET) Degraders Derived from Triazolodiazepine (JQ1) and Tetrahydroquinoline (I-BET726) BET Inhibitor Scaffolds. *J Med Chem.* **2018,** *61* (2), 504-513.
5. Sun, X.; Gao, H.; Yang, Y.; He, M.; Wu, Y.; Song, Y.; Tong, Y.; Rao, Y., PROTACs: great opportunities for academia and industry. *Signal Transduction and Targeted Therapy* **2019,** *4* (1), 64.
6. Pettersson, M.; Crews, C. M., PROteolysis TArgeting Chimeras (PROTACs) — Past, present and future. *Drug Discovery Today: Technol.* **2019,** *31*, 15-27.
7. Hanzl, A.; Winter, G. E., Targeted protein degradation: current and future challenges. *Curr. Opin. Chem. Biol.* **2020,** *56*, 35-41.
8. Bond, M. J.; Crews, C. M., Proteolysis targeting chimeras (PROTACs) come of age: entering the third decade of targeted protein degradation. *RSC Chemical Biology* **2021,** *2* (3), 725-742.
9. Zou, Y.; Ma, D.; Wang, Y., The PROTAC technology in drug development. *Cell Biochem Funct* **2019,** *37* (1), 21-30.
10. An, S.; Fu, L., Small-molecule PROTACs: An emerging and promising approach for the development of targeted therapy drugs. *EBioMedicine* **2018,** *36*, 553-562.
11. Hughes, Scott J.; Ciulli, A., Molecular recognition of ternary complexes: a new dimension in the structure-guided design of chemical degraders. *Essays in Biochemistry* **2017,** *61* (5), 505-516.
12. Bondeson, D. P.; Mares, A.; Smith, I. E.; Ko, E.; Campos, S.; Miah, A. H.; Mulholland, K. E.; Routly, N.; Buckley, D. L.; Gustafson, J. L.; Zinn, N.; Grandi, P.; Shimamura, S.; Bergamini, G.; Faelth-Savitski, M.; Bantscheff, M.; Cox, C.; Gordon, D. A.; Willard, R. R.; Flanagan, J. J.; Casillas, L. N.; Votta, B. J.; den Besten, W.; Famm, K.; Kruidenier, L.; Carter, P. S.; Harling, J. D.; Churcher, I.; Crews, C. M., Catalytic in vivo protein knockdown by small-molecule PROTACs. *Nat Chem Biol* **2015,** *11* (8), 611-7.
13. Bondeson, D. P.; Smith, B. E.; Burslem, G. M.; Buhimschi, A. D.; Hines, J.; Jaime-Figueroa, S.; Wang, J.; Hamman, B. D.; Ishchenko, A.; Crews, C. M., Lessons in PROTAC Design from Selective Degradation with a Promiscuous Warhead. *Cell Chem Biol.* **2018,** *25* (1), 78-87.e5.
14. Gadd, M. S.; Testa, A.; Lucas, X.; Chan, K.-H.; Chen, W.; Lamont, D. J.; Zengerle, M.; Ciulli, A., Structural basis of PROTAC cooperative recognition for selective protein degradation. *Nat Chem Biol* **2017,** *13* (5), 514-521.
15. Toure, M.; Crews, C. M., Small-Molecule PROTACS: New Approaches to Protein Degradation. *Angew Chem Int Ed Engl.* **2016,** *55* (6), 1966-1973.

16. Mullard, A., Arvinas's PROTACs pass first safety and PK analysis. *Nat Rev Drug Discov* **2019,** *18* (12), 895.
17. Petrylak, D. P.; Gao, X.; Vogelzang, N. J.; Garfield, M. H.; Taylor, I.; Dougan Moore, M.; Peck, R. A.; Burris, H. A., First-in-human phase I study of ARV-110, an androgen receptor (AR) PROTAC degrader in patients (pts) with metastatic castrate-resistant prostate cancer (mCRPC) following enzalutamide (ENZ) and/or abiraterone (ABI). *Journal of Clinical Oncology* **2020,** *38* (15_suppl), 3500-3500.
18. Lin, X.; Xiang, H.; Luo, G., Targeting estrogen receptor α for degradation with PROTACs: A promising approach to overcome endocrine resistance. *Eur. J. Med. Chem.* **2020,** *206*, 112689.
19. Cantrill, C.; Chaturvedi, P.; Rynn, C.; Petrig Schaffland, J.; Walter, I.; Wittwer, M. B., Fundamental aspects of DMPK optimization of targeted protein degraders. *Drug Discovery Today* **2020,** *25* (6), 969-982.
20. Churcher, I., Protac-Induced Protein Degradation in Drug Discovery: Breaking the Rules or Just Making New Ones? *J Med Chem.* **2018,** *61* (2), 444-452.
21. Liu, X.; Zhang, X.; Lv, D.; Yuan, Y.; Zheng, G.; Zhou, D., Assays and technologies for developing proteolysis targeting chimera degraders. *Future Med Chem.* **2020,** *12* (12), 1155-1179.
22. Ermondi, G.; Vallaro, M.; Caron, G., Degraders early developability assessment: face-to-face with molecular properties. *Drug Discovery Today* **2020,** *25* (9), 1585-1591.
23. Ermondi, G.; Garcia-Jimenez, D.; Caron, G., PROTACs and Building Blocks: The 2D Chemical Space in Very Early Drug Discovery. *Molecules* **2021,** *26* (3).
24. Watt, G. F.; Scott-Stevens, P.; Gaohua, L., Targeted protein degradation in vivo with Proteolysis Targeting Chimeras: Current status and future considerations. *Drug Discovery Today: Technologies* **2019,** *31*, 69-80.
25. Atilaw, Y.; Poongavanam, V.; Svensson Nilsson, C.; Nguyen, D.; Giese, A.; Meibom, D.; Erdelyi, M.; Kihlberg, J., Solution Conformations Shed Light on PROTAC Cell Permeability. *ACS Med. Chem. Lett.* **2021,** *12* (1), 107-114.
26. Edmondson, S. D.; Yang, B.; Fallan, C., Proteolysis targeting chimeras (PROTACs) in 'beyond rule-of-five' chemical space: Recent progress and future challenges. *Bioorganic & Medicinal Chemistry Letters* **2019,** *29* (13), 1555-1564.
27. Maple, H. J.; Clayden, N.; Baron, A.; Stacey, C.; Felix, R., Developing degraders: principles and perspectives on design and chemical space. *MedChemComm* **2019,** *10* (10), 1755-1764.
28. Matsson, P.; Kihlberg, J., How Big Is Too Big for Cell Permeability? *J Med Chem.* **2017,** *60* (5), 1662-1664.
29. Menichetti, R.; Kanekal, K. H.; Bereau, T., Drug–Membrane Permeability across Chemical Space. *ACS Central Science* **2019,** *5* (2), 290-298.
30. Doak, B. C.; Giordanetto, F.; Kihlberg, J., Review Oral Druggable Space beyond the Rule of 5 : Insights from Drugs and Clinical Candidates. *Chemistry and Biology* **2014,** *21*, 1115-1142.
31. Klein, V. G.; Townsend, C. E.; Testa, A.; Zengerle, M.; Maniaci, C.; Hughes, S. J.; Chan, K.-H.; Ciulli, A.; Lokey, R. S., Understanding and improving the membrane permeability of VH032-based PROTACs. *ACS Medicinal Chemistry Letters* **2020**.

32. Foley, C. A.; Potjewyd, F.; Lamb, K. N.; James, L. I.; Frye, S. V., Assessing the Cell Permeability of Bivalent Chemical Degraders Using the Chloroalkane Penetration Assay. *ACS Chem Biol.* **2020,** *15* (1), 290-295.
33. Scott, D. E.; Rooney, T. P. C.; Bayle, E. D.; Mirza, T.; Willems, H. M. G.; Clarke, J. H.; Andrews, S. P.; Skidmore, J., Systematic Investigation of the Permeability of Androgen Receptor PROTACs. *ACS Medicinal Chemistry Letters* **2020,** *11* (8), 1539-1547.
34. Roy, M. J.; Winkler, S.; Hughes, S. J.; Whitworth, C.; Galant, M.; Farnaby, W.; Rumpel, K.; Ciulli, A., SPR-Measured Dissociation Kinetics of PROTAC Ternary Complexes Influence Target Degradation Rate. *ACS Chem Biol.* **2019,** *14* (3), 361-368.
35. Smith, B. E.; Wang, S. L.; Jaime-Figueroa, S.; Harbin, A.; Wang, J.; Hamman, B. D.; Crews, C. M., Differential PROTAC substrate specificity dictated by orientation of recruited E3 ligase. *Nat Comm.* **2019,** *10* (1), 131.
36. Bai, N.; Miller, S. A.; Andrianov, G. V.; Yates, M.; Kirubakaran, P.; Karanicolas, J., Rationalizing PROTAC-Mediated Ternary Complex Formation Using Rosetta. *Journal of Chemical Information and Modeling* **2021**.
37. Bockus, A. T.; Schwochert, J. A.; Pye, C. R.; Townsend, C. E.; Sok, V.; Bednarek, M. A.; Lokey, R. S., Going Out on a Limb: Delineating The Effects of β-Branching, N-Methylation, and Side Chain Size on the Passive Permeability, Solubility, and Flexibility of Sanguinamide A Analogues. *J Med Chem.* **2015,** *58* (18), 7409-7418.
38. Raina, K.; Lu, J.; Qian, Y.; Altieri, M.; Gordon, D.; Rossi, A. M. K.; Wang, J.; Chen, X.; Dong, H.; Siu, K.; Winkler, J. D.; Crew, A. P.; Crews, C. M.; Coleman, K. G., PROTAC-induced BET protein degradation as a therapy for castration-resistant prostate cancer. *Proc Natl Acad Sci U S A* **2016,** *113* (26), 7124-7129.
39. Arnott, J. A.; Planey, S. L., The influence of lipophilicity in drug discovery and design. *Expert Opinion on Drug Discovery* **2012,** *7* (10), 863-875.
40. Waring, M. J., Lipophilicity in drug discovery. *Expert Opinion on Drug Discovery* **2010,** *5* (3), 235-248.
41. Naylor, M. R.; Ly, A. M.; Handford, M. J.; Ramos, D. P.; Pye, C. R.; Furukawa, A.; Klein, V. G.; Noland, R. P.; Edmondson, Q.; Turmon, A. C.; Hewitt, W. M.; Schwochert, J.; Townsend, C. E.; Kelly, C. N.; Blanco, M.-J.; Lokey, R. S., Lipophilic Permeability Efficiency Reconciles the Opposing Roles of Lipophilicity in Membrane Permeability and Aqueous Solubility. *J Med Chem.* **2018,** *61* (24), 11169-11182.
42. Galdeano, C.; Gadd, M. S.; Soares, P.; Scaffidi, S.; Van Molle, I.; Birced, I.; Hewitt, S.; Dias, D. M.; Ciulli, A., Structure-Guided Design and Optimization of Small Molecules Targeting the Protein–Protein Interaction between the von Hippel–Lindau (VHL) E3 Ubiquitin Ligase and the Hypoxia Inducible Factor (HIF) Alpha Subunit with in Vitro Nanomolar Affinities. *J. Med. Chem.* **2014,** *57* (20), 8657-8663.
43. Avdeef, A., The rise of PAMPA. *Expert Opinion on Drug Metabolism & Toxicology* **2005,** *1* (2), 325-342.
44. Hann, M. M.; Simpson, G. L., Intracellular drug concentration and disposition – The missing link? *Methods* **2014,** *68* (2), 283-285.
45. Liu, Q.; Hou, J.; Chen, X.; Liu, G.; Zhang, D.; Sun, H.; Zhang, J., P-Glycoprotein Mediated Efflux Limits the Transport of the Novel Anti-Parkinson's Disease Candidate Drug FLZ across the Physiological and PD Pathological In Vitro BBB Models. *PLOS ONE* **2014,** *9* (7), e102442.

46. Shultz, M. D., Two Decades under the Influence of the Rule of Five and the Changing Properties of Approved Oral Drugs. *J Med Chem.* **2019,** *62* (4), 1701-1714.
47. Winiwarter, S.; Ax, F.; Lennernäs, H.; Hallberg, A.; Pettersson, C.; Karlén, A., Hydrogen bonding descriptors in the prediction of human in vivo intestinal permeability. *Journal of Molecular Graphics and Modelling* **2003,** *21* (4), 273-287.
48. Biron, E.; Chatterjee, J.; Ovadia, O.; Langenegger, D.; Brueggen, J.; Hoyer, D.; Schmid, H. A.; Jelinek, R.; Gilon, C.; Hoffman, A.; Kessler, H., Improving Oral Bioavailability of Peptides by Multiple N-Methylation: Somatostatin Analogues. *Angew Chem Int Ed Engl.* **2008,** *47* (14), 2595-2599.
49. Ovadia, O.; Greenberg, S.; Chatterjee, J.; Laufer, B.; Opperer, F.; Kessler, H.; Gilon, C.; Ho, A., The Effect of Multiple N-Methylation on Intestinal Permeability of Cyclic Hexapeptides. *Molecular Pharmaceutics* **2011,** *8*, 479-487.
50. Wang, C. K.; Northfield, S. E.; Colless, B.; Chaousis, S.; Hamernig, I.; Lohman, R.-J.; Nielsen, D. S.; Schroeder, C. I.; Liras, S.; Price, D. A.; Fairlie, D. P.; Craik, D. J., Rational design and synthesis of an orally bioavailable peptide guided by NMR amide temperature coefficients. *Proc Natl Acad Sci U S A.* **2014,** *111* (49), 17504-17509.
51. Rezai, T.; Bock, J. E.; Zhou, M. V.; Kalyanaraman, C.; Lokey, R. S.; Jacobson, M. P., Conformational Flexibility, Internal Hydrogen Bonding, and Passive Membrane Permeability: Successful in Silico Prediction of the Relative Permeabilities of Cyclic Peptides. *J Am Chem Soc.* **2006,** *128* (43), 14073-14080.
52. Thansandote, P.; Harris, R. M.; Dexter, H. L.; Simpson, G. L.; Pal, S.; Upton, R. J.; Valko, K., Improving the passive permeability of macrocyclic peptides : Balancing permeability with other physicochemical properties. *Bioorg Med Chem.* **2015,** *23* (2), 322-327.
53. Leeson, P. D.; Springthorpe, B., The influence of drug-like concepts on decision-making in medicinal chemistry. *Nat Rev Drug Discov.* **2007,** *6* (11), 881-890.
54. Cyrus, K.; Wehenkel, M.; Choi, E.-y.; Han, H.-j.; Lee, H.; Kim, K.-b., Impact of linker length on the activity of PROTACs. *Molecular BioSystems* **2011,** *7*, 359-364.
55. Wang, Y.; Jiang, X.; Feng, F.; Liu, W.; Sun, H., Degradation of proteins by PROTACs and other strategies. *Acta Pharmaceutica Sinica B* **2020,** *10* (2), 207-238.
56. Abraham, M. H.; Chadha, H. S.; Whiting, G. S.; Mitchell, R. C., Hydrogen bonding. 32. An analysis of water-octanol and water-alkane partitioning and the delta log P parameter of seiler. *J Pharm Sci* **1994,** *83* (8), 1085-100.
57. Shalaeva, M.; Caron, G.; Abramov, Y. A.; O'Connell, T. N.; Plummer, M. S.; Yalamanchi, G.; Farley, K. A.; Goetz, G. H.; Philippe, L.; Shapiro, M. J., Integrating Intramolecular Hydrogen Bonding (IMHB) Considerations in Drug Discovery Using ΔlogP As a Tool. *J Med Chem.* **2013,** *56* (12), 4870-4879.
58. Caron, G.; Vallaro, M.; Ermondi, G., Log P as a tool in intramolecular hydrogen bond considerations. *Drug Discovery Today: Technologies* **2018,** *27*, 65-70.
59. Gadd, M. S.; Testa, A.; Lucas, X.; Chan, K.-H.; Chen, W.; Lamont, D. J.; Zengerle, M.; Ciulli, A., Structural basis of PROTAC cooperative recognition for selective protein degradation. *Nat. Chem. Biol.* **2017,** *13* (5), 514-521.
60. Soares, P.; Gadd, M. S.; Frost, J.; Galdeano, C.; Ellis, L.; Epemolu, O.; Rocha, S.; Read, K. D.; Ciulli, A., Group-Based Optimization of Potent and Cell-Active Inhibitors of the von Hippel–Lindau (VHL) E3 Ubiquitin Ligase: Structure–Activity Relationships Leading to the Chemical Probe (2S,4R)-1-((S)-2-(1-Cyanocyclopropanecarboxamido)-3,3-dimethylbutanoyl)-4-

hydroxy-N-(4-(4-methylthiazol-5-yl)benzyl)pyrrolidine-2-carboxamide (VH298). *J Med Chem.* **2018,** *61* (2), 599-618.
61. Ouellette, R. J.; Rawn, J. D., 22 - Carboxylic Acid Derivatives. In *Organic Chemistry (Second Edition)*, Ouellette, R. J.; Rawn, J. D., Eds. Academic Press: 2018; pp 665-710.
62. Filippakopoulos, P.; Qi, J.; Picaud, S.; Shen, Y.; Smith, W. B.; Fedorov, O.; Morse, E. M.; Keates, T.; Hickman, T. T.; Felletar, I.; Philpott, M.; Munro, S.; McKeown, M. R.; Wang, Y.; Christie, A. L.; West, N.; Cameron, M. J.; Schwartz, B.; Heightman, T. D.; La Thangue, N.; French, C. A.; Wiest, O.; Kung, A. L.; Knapp, S.; Bradner, J. E., Selective inhibition of BET bromodomains. *Nature* **2010,** *468* (7327), 1067-1073.
63. Filippakopoulos, P.; Qi, J.; Picaud, S.; Shen, Y.; Smith, W. B.; Fedorov, O.; Morse, E. M.; Keates, T.; Hickman, T. T.; Felletar, I.; Philpott, M.; Munro, S.; McKeown, M. R.; Wang, Y.; Christie, A. L.; West, N.; Cameron, M. J.; Schwartz, B.; Heightman, T. D.; La Thangue, N.; French, C. A.; Wiest, O.; Kung, A. L.; Knapp, S.; Bradner, J. E., Selective inhibition of BET bromodomains. *Nature* **2010,** *468*, 1067-73.
64. Nicodeme, E.; Jeffrey, K. L.; Schaefer, U.; Beinke, S.; Dewell, S.; Chung, C.-w.; Chandwani, R.; Marazzi, I.; Wilson, P.; Coste, H.; White, J.; Kirilovsky, J.; Rice, C. M.; Lora, J. M.; Prinjha, R. K.; Lee, K.; Tarakhovsky, A., Suppression of inflammation by a synthetic histone mimic. *Nature* **2010,** *468*, 1119.
65. Chung, C.-w.; Coste, H.; White, J. H.; Mirguet, O.; Wilde, J.; Gosmini, R. L.; Delves, C.; Magny, S. M.; Woodward, R.; Hughes, S. A.; Boursier, E. V.; Flynn, H.; Bouillot, A. M.; Bamborough, P.; Brusq, J.-M. G.; Gellibert, F. J.; Jones, E. J.; Riou, A. M.; Homes, P.; Martin, S. L.; Uings, I. J.; Toum, J.; Clément, C. A.; Boullay, A.-B.; Grimley, R. L.; Blandel, F. M.; Prinjha, R. K.; Lee, K.; Kirilovsky, J.; Nicodeme, E., Discovery and Characterization of Small Molecule Inhibitors of the BET Family Bromodomains. *J Med Chem.* **2011,** *54* (11), 3827-3838.
66. Wang, C. K.; Northfield, S. E.; Swedberg, J. E.; Colless, B.; Chaousis, S.; Price, D. A.; Liras, S.; Craik, D. J., Exploring experimental and computational markers of cyclic peptides: Charting islands of permeability. *European Journal of Medicinal Chemistry* **2015,** *97*, 202-213.
67. Pye, C. R.; Hewitt, W. M.; Schwochert, J.; Haddad, T. D.; Townsend, C. E.; Etienne, L.; Lao, Y.; Limberakis, C.; Furukawa, A.; Mathiowetz, A. M.; Price, D. A.; Liras, S.; Lokey, R. S., Nonclassical Size Dependence of Permeation Defines Bounds for Passive Adsorption of Large Drug Molecules. *J Med Chem.* **2017,** *60* (5), 1665-1672.
68. Furukawa, A.; Townsend, C. E.; Schwochert, J.; Pye, C. R.; Bednarek, M. A.; Lokey, R. S., Passive Membrane Permeability in Cyclic Peptomer Scaffolds Is Robust to Extensive Variation in Side Chain Functionality and Backbone Geometry. *J Med Chem.* **2016,** *59* (20), 9503-9512.
69. Testa, A.; Hughes, S. J.; Lucas, X.; Wright, J. E.; Ciulli, A., Structure-Based Design of a Macrocyclic PROTAC. *Angew Chem Int Ed Engl.* **2020,** *59* (4), 1727-1734.
70. Douglass, E. F., Jr.; Miller, C. J.; Sparer, G.; Shapiro, H.; Spiegel, D. A., A comprehensive mathematical model for three-body binding equilibria. *J. Am. Chem. Soc.* **2013,** *135* (16), 6092-9.
71. Riching, K. M.; Mahan, S.; Corona, C. R.; McDougall, M.; Vasta, J. D.; Robers, M. B.; Urh, M.; Daniels, D. L., Quantitative Live-Cell Kinetic Degradation and Mechanistic Profiling of PROTAC Mode of Action. *ACS Chem Biol.* **2018,** *13* (9), 2758-2770.
72. Zoppi, V.; Hughes, S. J.; Maniaci, C.; Testa, A.; Gmaschitz, T.; Wieshofer, C.; Koegl, M.; Riching, K. M.; Daniels, D. L.; Spallarossa, A.; Ciulli, A., Iterative Design and Optimization of Initially Inactive Proteolysis Targeting Chimeras (PROTACs) Identify VZ185 as a Potent,

Fast, and Selective von Hippel-Lindau (VHL) Based Dual Degrader Probe of BRD9 and BRD7. *J Med Chem* **2019,** *62* (2), 699-726.
73. Farnaby, W.; Koegl, M.; Roy, M. J.; Whitworth, C.; Diers, E.; Trainor, N.; Zollman, D.; Steurer, S.; Karolyi-Oezguer, J.; Riedmueller, C.; Gmaschitz, T.; Wachter, J.; Dank, C.; Galant, M.; Sharps, B.; Rumpel, K.; Traxler, E.; Gerstberger, T.; Schnitzer, R.; Petermann, O.; Greb, P.; Weinstabl, H.; Bader, G.; Zoephel, A.; Weiss-Puxbaum, A.; Ehrenhöfer-Wölfer, K.; Wöhrle, S.; Boehmelt, G.; Rinnenthal, J.; Arnhof, H.; Wiechens, N.; Wu, M.-Y.; Owen-Hughes, T.; Ettmayer, P.; Pearson, M.; McConnell, D. B.; Ciulli, A., BAF complex vulnerabilities in cancer demonstrated via structure-based PROTAC design. *Nat Chem Biol.* **2019,** *15* (7), 672-680.
74. Hu, J.; Hu, B.; Wang, M.; Xu, F.; Miao, B.; Yang, C. Y.; Wang, M.; Liu, Z.; Hayes, D. F.; Chinnaswamy, K.; Delproposto, J.; Stuckey, J.; Wang, S., Discovery of ERD-308 as a Highly Potent Proteolysis Targeting Chimera (PROTAC) Degrader of Estrogen Receptor (ER). *J Med Chem* **2019,** *62* (3), 1420-1442.
75. Young, R. J.; Green, D. V. S.; Luscombe, C. N.; Hill, A. P., Getting physical in drug discovery II: the impact of chromatographic hydrophobicity measurements and aromaticity. *Drug discovery today* **2011,** *16* (17-18), 822-830.
76. Cromm, P. M.; Samarasinghe, K. T. G.; Hines, J.; Crews, C. M., Addressing Kinase-Independent Functions of Fak via PROTAC-Mediated Degradation. *J Am Chem Soc.* **2018,** *140* (49), 17019-17026.
77. Costales, M. G.; Suresh, B.; Vishnu, K.; Disney, M. D., Targeted Degradation of a Hypoxia-Associated Non-coding RNA Enhances the Selectivity of a Small Molecule Interacting with RNA. *Cell Chem Biol.* **2019,** *26* (8), 1180-1186.e5.
78. Siriwardena, S. U.; Munkanatta Godage, D. N. P.; Shoba, V. M.; Lai, S.; Shi, M.; Wu, P.; Chaudhary, S. K.; Schreiber, S. L.; Choudhary, A., Phosphorylation-Inducing Chimeric Small Molecules. *J Am Chem Soc.* **2020,** *142* (33), 14052-14057.
79. Takahashi, D.; Moriyama, J.; Nakamura, T.; Miki, E.; Takahashi, E.; Sato, A.; Akaike, T.; Itto-Nakama, K.; Arimoto, H., AUTACs: Cargo-Specific Degraders Using Selective Autophagy. *Mol Cell.* **2019,** *76* (5), 797-810.e10.

Table of contents graphic: